



Precise spiking motifs in neurobiological and neuromorphic data [1]

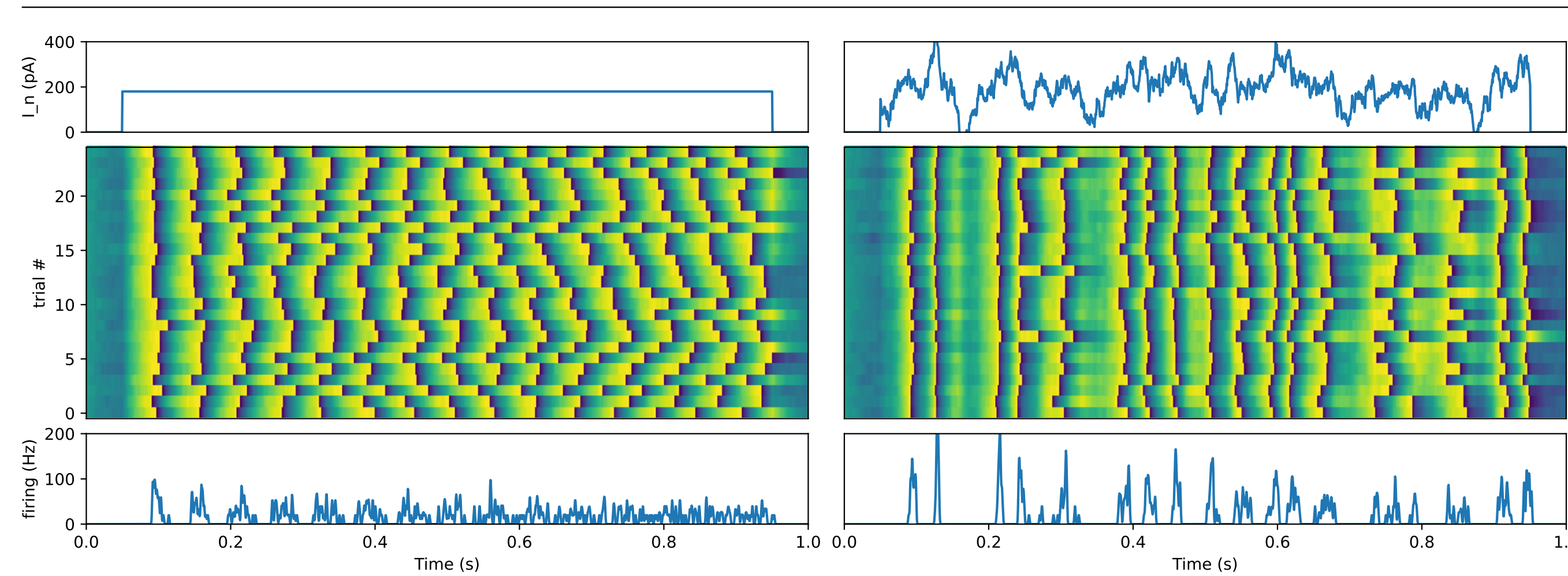


Figure 1. Reproducibility of the spiking response of a biological neuron. The timing of the spikes produced following the repetition of a step stimulus is less reproducible than that to a noisy stimulus. The stimulus current value over time for a step stimulus (top left) and for a noisy one (top right). Trial repetitions of a leaky integrate-and-fire neuron stimulated by the stimulus on the upper row (middle row). Membrane potential is represented by dark blue color when low and with yellow colors when depolarized and we show the average firing rate across trials (lower row). While this seems paradoxical at first sight, it highlights the consequence of using the same frozen noise at each repetition and highlights the highly reproducible pattern of spikes when it is driven by a highly dynamic input. Run this [online notebook](#) for a replication of the results from [2] using a simple LIF model.

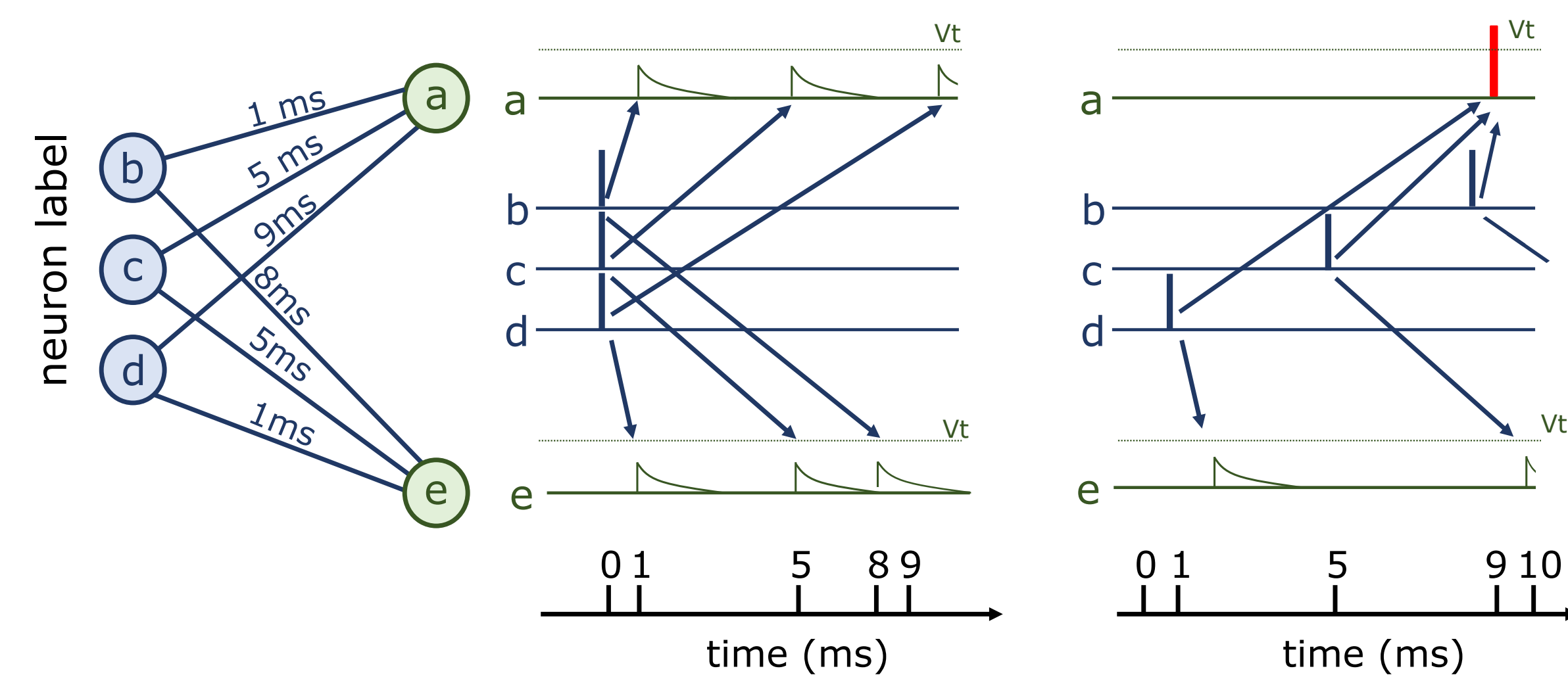


Figure 2. Core mechanism of polychrony detection [3]. (Left) In this example, three presynaptic neurons denoted b , c and d are fully connected to two post-synaptic neurons a and e , with different delays of respectively 1, 5, and 9 ms for a and 8, 5, and 1 ms for e . (Middle) If three spikes are emitted synchronously from the presynaptic neurons, this will generate post-synaptic potentials that will reach a and e asynchronously because of the heterogeneous delays, and they may not be sufficient to reach the membrane threshold in either of the post-synaptic neurons; therefore, no spike will be emitted. (Right) If the pulses are emitted from presynaptic neurons such that, taking into account the delays, they reach the post-synaptic neuron a at the same time (here, at $t = 10$ ms), the post-synaptic potentials evoked by the three pre-synaptic neurons sum up, causing the voltage threshold to be crossed and thus to the emission of an output spike (red color), while none is emitted from post-synaptic neuron e .

Acknowledgments

This research was funded by ANR project AgileNeuRobot ANR-20-CE23-0021 (<https://laurentperrinet.github.io/grant/anr-anr>) and from A*Midex grant "Polychronies" number AMX-21-RID-025 (<https://laurentperrinet.github.io/grant/polychronies>).

Heterogeneous Delays Spiking Neural Network (HD-SNN) [4]

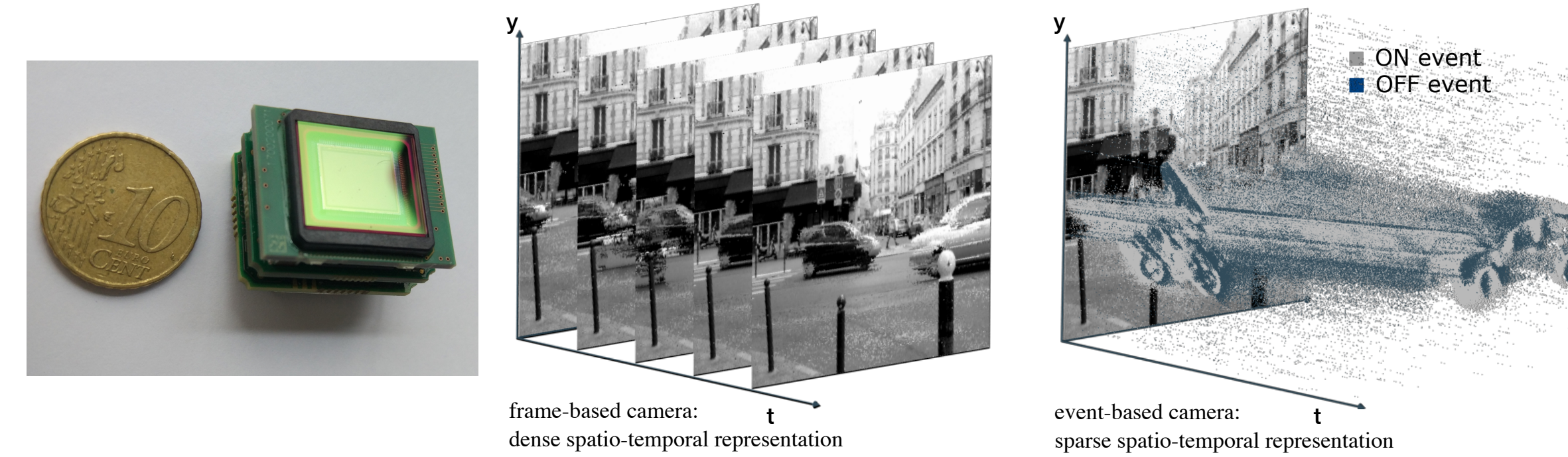


Figure 3. Event-based cameras. A miniature ATIS sensor. Contrary to a classical frame-based camera for which a full dense image representation is given at discrete, regularly spaced timings, the event-based camera provides with events at the micro-second resolution. These are sparse as they represent luminance increments or decrements (ON and OFF events, respectively).

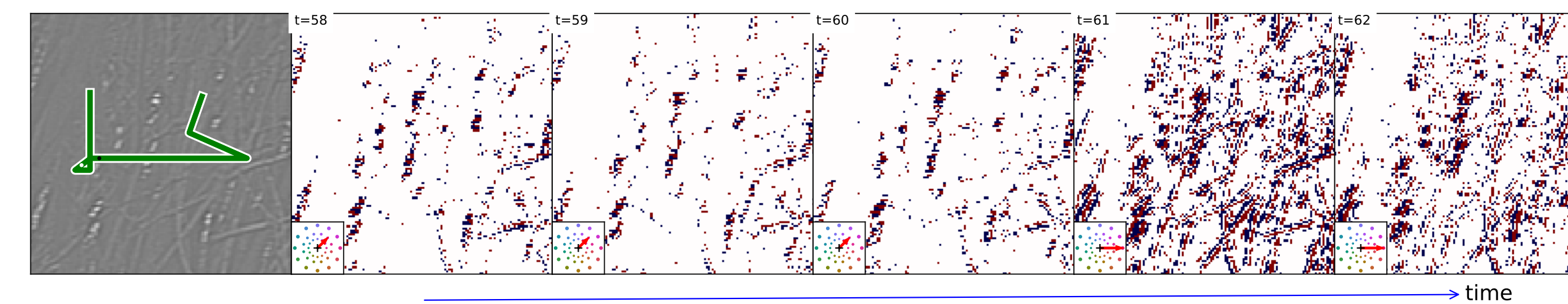


Figure 4. Motion Detection Task. To generate realistic event-based dynamic scenes, we mimic the effect of minute saccadic eye movements on a large natural scene (1024×1024) by extracting an image (128×128) which center is moving dynamically according to a jagged random walk. (Left) We show an instance of this trajectory (with a length of 200 ms, green line) superimposed on the luminance contrasts observed at time step $t = 15$ ms. (Right) The dynamics of this image, translated according to the saccadic trajectory, produces a naturalistic movie, which is then transformed into an event-based representation. We show snapshots of the resulting synthetic event stream at different time steps (from $t = 15$ ms to $t = 19$ ms, these frames are marked on the trajectory by a white and black dot, respectively). Mimicking the response of ganglion cells in the retina, this representation encodes at each pixel all-or-none increases or decreases in luminance, i.e., ON (red) and OFF (blue) spikes. In the lower left corner of the snapshots, we show the corresponding instantaneous motion vector (red arrow).



Figure 5. Representation of the weights for 8 directions for a single speed (among the 12×3 different kernels of the model) as learned on the dataset of naturalistic scenes. The directions are shown as red arrows in the left insets, where the disks correspond to the set of different possible motions. The spatiotemporal kernels are shown as slices of spatial weights at different delays. Delays vary along the horizontal axis from the far right (delay of one step) to the left (up to a delay of 12 steps, the remaining synapses being not represented).

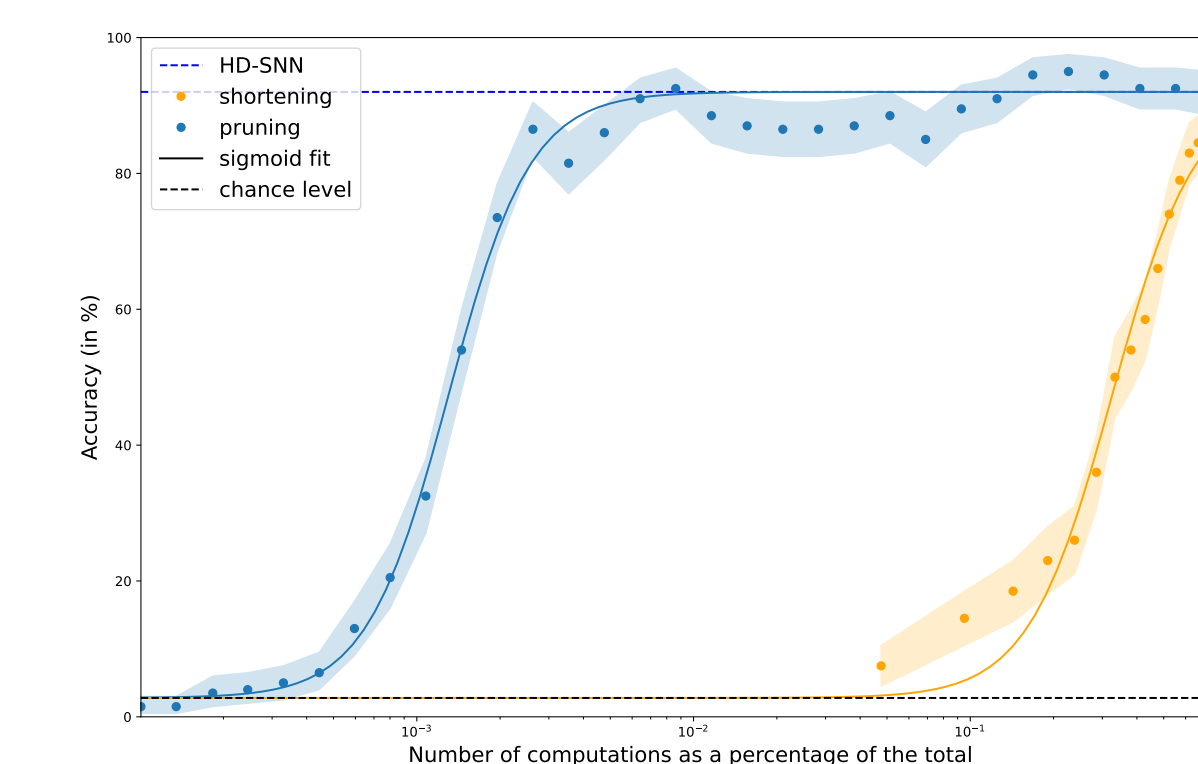


Figure 6. Accuracy as a function of computational load for the HD-SNN model (blue dots) with error bars indicating the 5% - 95% quantiles. The relative computational load (on a logarithmic axis) is controlled by changing the percentage of nonzero weights relative to the dense convolution kernel. If we use only the weights at the shortest delays, the accuracy quickly drops. However, if we prune the lowest coefficients, we observe a stable accuracy value, with a half-saturation observed at ≈ 670 less computations.

Detection of Spiking Motifs by Learning a HD-SNN [5]

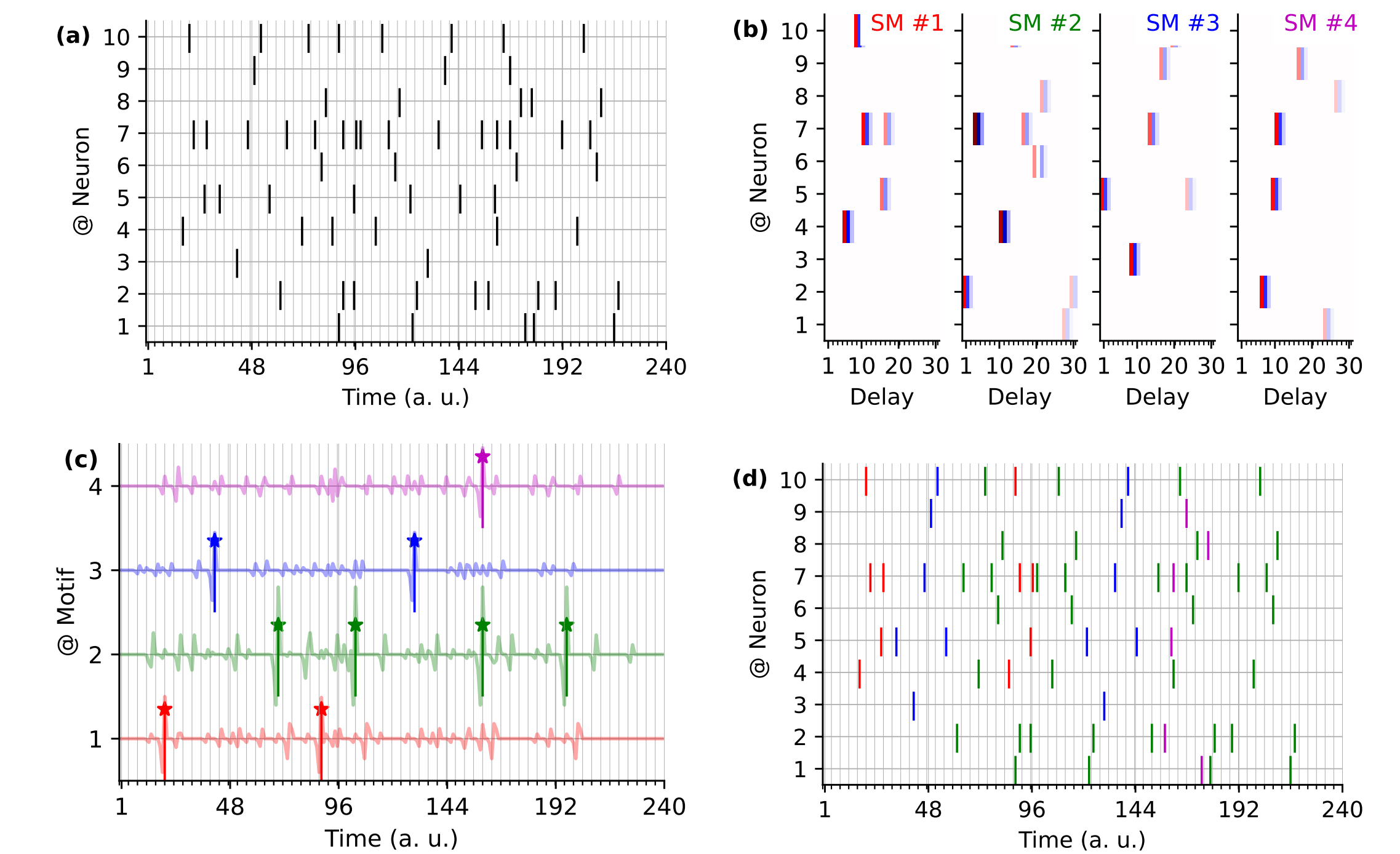


Figure 7. From generating raster plots to inferring spiking motifs. We derive a detection model as the optimal inversion of a generative model for spike generation. (a) As an illustration for the generative model, we draw a multiunit raster plot synthesized from 4 different spiking motifs (SMs) and for 10 presynaptic neurons. (b) We show these motifs, each identified at the top by a different color. The evidence of activation (red) or deactivation (blue) is assigned to each presynaptic neuron and 31 different possible delays. (c) The activation in time of the different motifs (denoted by stars) is drawn at random and then used to generate a raster plot on the multi-unit address space (see panel a). By inverting this model, an inference model can be defined for their efficient detection, outputting an evidence value (continuous line) from which the identity and timing of SMs can be inferred (vertical bars). (d) The original raster plot can be annotated with each identified spiking motif (as represented by the respective colors).

References

- [1] Antoine Grimaldi et al. "Precise spiking motifs in neurobiological and neuromorphic data". In: *Brain Sciences* (2022). DOI: 10.3390/brainsci13010068. URL: <https://laurentperrinet.github.io/publication/grimaldi-22-polychronies/>.
- [2] Zachary F. Mainen and Terrence J. Sejnowski. "Reliability of Spike Timing in Neocortical Neurons". en. In: *Science* 268.5216 (June 1995), pp. 1503–1506. ISSN: 0036-8075, 1095-9203. DOI: 10.1126/science.7770778.
- [3] Eugene M. Izhikevich. "Polychronization: Computation with Spikes". In: *Neural Computation* 18.2 (Feb. 2006), pp. 245–282. ISSN: 0899-7667. DOI: 10.1162/089976606775093882.
- [4] Antoine Grimaldi and Laurent U Perrinet. "Learning heterogeneous delays in a layer of spiking neurons for fast motion detection". In: *Biological Cybernetics* (2023). URL: <https://laurentperrinet.github.io/publication/grimaldi-23-bc/>.
- [5] Laurent U Perrinet. "Accurate Detection of Spiking Motifs by Learning Heterogeneous Delays of a Spiking Neural Network". In: *ICANN 2023 - Special Session on Recent Advances in Spiking Neural Networks*. Heraklion (Crete, Greece), Sept. 27, 2023. URL: <https://laurentperrinet.github.io/publication/perrinet-23-icann/>.
- [6] Adrien Fois and Laurent U Perrinet. "Self-Supervised Learning of Spiking Motifs in Neurobiological Data". In: *FENS Forum 2024*. Vienna (Austria), June 27, 2024. URL: <https://laurentperrinet.github.io/publication/fois-24-fens/>.